Inclusion of screening effects in the van der Waals corrected DFT simulation of adsorption processes on metal surfaces

Pier Luigi Silvestrelli and Alberto Ambrosetti*

Dipartimento di Fisica e Astronomia, Università di Padova, via Marzolo 8, I–35131, Padova, Italy, and DEMOCRITOS National Simulation Center of the Italian Istituto Officina dei Materiali (IOM) of the Italian National Research Council (CNR), Trieste, Italy

(Received 9 December 2012; revised manuscript received 21 January 2013; published 4 February 2013)

The DFT/vdW-WF2 method, recently developed to include the van der Waals (vdW) interactions in density functional theory (DFT) using the maximally localized Wannier functions, is improved by taking into account screening effects and applied to the study of adsorption of rare gases and small molecules, H_2, CH_4, and H_2O on the Cu(111) metal surface, and of H_2 on Al(111), and Xe on Pb(111), which are all cases where screening effects are expected to be important. Screening is included in DFT/vdW-WF2 by following different recipes, also considering the single-layer approximation adopted to mimic a screened metal substrate. Comparison of the computed equilibrium binding energies and distances, and the C_3 coefficients characterizing the adparticle-surface van der Waals interactions, with available experimental and theoretical reference data show that the improvement with respect to the original unscreened approach is remarkable. The results are also compared with those obtained by other vdW-corrected DFT schemes.

DOI: 10.1103/PhysRevB.87.075401 PACS number(s): 68.43.Bc, 71.15.Mb, 68.35.Md

I. INTRODUCTION

Adsorption processes on solid surfaces represent a very important topic both from a fundamental point of view and to design and optimize countless material applications. In particular, the adsorption of closed electron-shell particles, such as rare-gas (RG) atoms, H_2, and methane (CH_4) molecules on metal surfaces is prototypical[1] for "physisorption" processes, characterized by an equilibrium between attractive, long-range van der Waals (vdW) interactions and short-range Pauli repulsion acting between the electronic charge densities of the substrate and the adsorbed atoms and molecules,[2] hereafter referred to as "adparticles."

RG adsorption on many close-packed metal surfaces, such as Ag(111), Al(111), Cu(111), Pd(111), Pt(111), etc., have been extensively studied both experimentally[3–6] and theoretically.[6–15] In spite of this recent substantial progress, the understanding of the interaction of RGs with metal surfaces is not complete yet.[6] For instance, due to the nondirectional character of the vdW interactions that should be dominant in physisorption processes, surface sites that maximize the coordination of the RG adsorbate atom were expected to be the preferred ones, so that it was usually assumed that the adsorbate occupies the maximally coordinated *hollow* site. However, this picture has been questioned by many experimental[3–5] and theoretical[8–11] recent studies, which indicate that the actual scenario is more complex: in particular, for Xe and Kr, a general tendency is found[6,8–11] for adsorption on metallic surfaces in the low-coordination *top* sites (this behavior was attributed[6,16] to the delocalization of charge density that increases the Pauli repulsion effect at the *hollow* sites relative to the *top* site and lifts the potential well upwards both in energy and height).

H_2 represents another interesting case; in fact, particularly for the H_2 molecule on low-index Cu surfaces, accurate physisorption data from experiment are available. Actually, H_2 is the only molecule for which a detailed mapping of the gas-surface interaction potential has been performed with resonance scattering measurements (see Ref. 17 and references therein).

We also consider the methane molecule (CH_4) on Cu(111), as representative of the interaction of an organic molecule with a metal substrate. Metal-organic interfaces are relevant for many applications, ranging from surface-functionalization processes, chemical sensors, coating, catalysts to organic electronics, organic field effect transistors, and organic spin-based devices (see, for instance, Ref. 18 and references therein).

Finally, we study the case of H_2O on Cu(111). In fact, water adsorption at well-defined single-crystal metal surfaces represent an important topic[19] because it is relevant to many areas of science: water is involved in many catalytic surface reactions and plays a crucial role in understanding wetting and corrosion, while environmental concerns underlie the increasing importance of the fuel cell reaction and interest in photocatalysis. In the case of the water molecule, differently from the other cases, the bonding with the metal surface is not only due to vdW interactions: in fact, a weak covalent bond is formed since water tends to act as an electron donor and the substrate as an electron acceptor[20] (typically H_2O donates a charge of about $0.1e$ to the metal[21]); moreover, the water molecule is characterized by a significant intrinsic electronic dipole moment, so that electrostatic effects are also important due to the interaction between the H_2O permanent dipole and its image beneath the surface.[21]

Density functional theory (DFT) is a well-established computational approach to study the structural and electronic properties of condensed matter systems from first principles and, in particular, to elucidate complex surface processes such as adsorptions, catalytic reactions, and diffusive motions. Although current density functionals are able to describe quantitatively condensed matter systems at much lower computational cost than other first-principles methods, they fail[22] to properly describe dispersion interactions. Dispersion forces originate from correlated charge oscillations in separate

fragments of matter and the most important component is represented by the R^{-6} vdW interaction,[23] originating from correlated instantaneous dipole fluctuations, which plays a fundamental role in adsorption processes of fragments weakly interacting with a substrate ("physisorbed").

This is clearly the case for the present systems, which can be divided into well separated fragments (adparticles and the metal substrate) with negligible electron-density overlap. The local or semilocal character of the most commonly employed exchange-correlation functionals makes DFT methods unable to correctly predict binding energies and equilibrium distances within both the local density (LDA) and the generalized gradient (GGA) approximations.[24] Typically, in many physisorbed systems, GGAs give only a shallow and flat adsorption well at large adparticle-substrate separations, while the LDA binding energy often turns out to be not far from the experimental adsorption energy; however, since it is well known that LDA tends to overestimate the binding in systems with inhomogeneous electron density (and to underestimate the equilibrium distances), the reasonable performances of LDA must be considered as accidental. Therefore a theoretical approach beyond the DFT-LDA/GGA framework, that is able to properly describe vdW effects is required to provide more quantitative results.[9]

In the last few years, a variety of practical methods have been proposed to make DFT calculations able to accurately describe vdW effects (for a recent review, see, for instance, Refs. 24–26). We have previously investigated by such an approach, namely the DFT/vdW-WF method[27–29] based on the use of maximally localized Wannier functions (MLWFs),[30] the interaction of the adsorption of RG atoms on the Cu(111) and Pb(111) surfaces.[31] However, in previous studies, screening effects, which are expected to be of importance in describing interactions of small molecules with metal surfaces[26,32–34] have been neglected[35] or taken into account only in a very approximate way.[31] In particular, for noble-metal surfaces, such as the Cu(111) one, given the high valence-electron density, screening effects are certainly relevant. In Ref. 31, we applied the DFT/vdW-WF method and approximated the screening effect by explicitly considering only the more localized MLWFs corresponding to the d-like orbitals, while the s- and p-like electrons were supposed to give a screening-effect contribution which was evaluated by a simple Thomas-Fermi model.

Here, we improve the previous approach to describe adsorption on metal surfaces in two basic ways. First, we use the new DFT/vdW-WF2 method,[36] which is based on the London expression and takes into account the intrafragment overlap of the MLWFs, leading to a considerable improvement not only in the evaluation of the C_6 vdW coefficients but also of the C_3 coefficients, characterizing molecule-surfaces vdW interactions.[36] Secondly, we describe screening effects more accurately, by adopting three different recipes, as detailed in the Method section.

We apply these new schemes to the case of adsorption of RGs and small molecules, H_2, CH_4, and H_2O on the Cu(111) metal surface, and of H_2 on Al(111), and Xe on Pb(111). In particular, the Cu(111) surface has been chosen because of the many experimental and theoretical data available which can be compared with ours in such a way to validate the present approach, whose performances are also compared with those of other vdW-corrected DFT schemes.

II. METHOD

Basically (more details can be found in Ref. 36), while in the original DFT/vdW-WF method the vdW energy correction for two separate fragments was computed using the exchange-correlation functional proposed by Andersson *et al.*,[37] the latest DFT/vdW-WF2 version is instead based on the simpler, well known London's expression[23] where two interacting atoms, A and B, are approximated by coupled harmonic oscillators and the vdW energy is taken to be the change of the zero-point energy of the coupled oscillations as the atoms approach; if only a single excitation frequency is associated to each atom, ω_A, ω_B, then

$$E_{\rm vdW}^{\rm London} = -\frac{3e^4}{2m^2}\frac{Z_A Z_B}{\omega_A\omega_B(\omega_A+\omega_B)}\frac{1}{R_{AB}^6}, \qquad (1)$$

where $Z_{A,B}$ is the total charge of A and B, and R_{AB} is the distance between the two atoms (e and m are the electronic charge and mass). This approach is clearly applicable to well separated fragments only: in the present systems, characterized by the interaction of adparticles weakly interacting with the substrate ("physisorbed"), this condition is always satisfied.

Now, adopting a simple classical theory of the atomic polarizability, the polarizability of an electronic shell of charge eZ_i and mass mZ_i, tied to a heavy undeformable ion can be written as

$$\alpha_i \simeq \frac{Z_i e^2}{m\omega_i^2}. \qquad (2)$$

Then, given the direct relation between polarizability and atomic volume,[38] we assume that $\alpha_i \sim \gamma S_i^3$, where γ is a proportionality constant, so that the atomic volume is expressed in terms of the MLWF spread S_i. Rewriting Eq. (1) in terms of the quantities defined above, one obtains an explicit expression (much simpler than the multidimensional integrals involved in the Andersson functional[37]) for the C_6 vdW coefficient:

$$C_6^{AB} = \frac{3}{2}\frac{\sqrt{Z_A Z_B}S_A^3 S_B^3\gamma^{3/2}}{\left(\sqrt{Z_B}S_A^{3/2}+\sqrt{Z_A}S_B^{3/2}\right)}. \qquad (3)$$

The constant γ can then be set up by imposing that the exact value for the H atom polarizability ($\alpha_H = 4.5$ a.u.) is obtained (of course, in the H case, one knows the exact analytical spread, $S_i = S_H = \sqrt{3}$ a.u.).

In order to achieve a better accuracy, one must properly deal with *intrafragment* MLWF overlap (we refer here to charge overlap, not to be confused with wave functions overlap): in fact, the DFT/vdW-WF method is strictly valid for nonoverlapping fragments only; now, while the overlap between the MLWFs relative to separated fragments is usually negligible for all the fragment separation distances of interest, the same is not true for the MLWFs belonging to the same fragment, which are often characterized by a significant overlap. This overlap affects the effective orbital volume, the polarizability, and the excitation frequency [see Eq. (2)], thus leading to a quantitative effect on the value of the C_6 coefficient. We take into account the effective change in

volume due to intrafragment MLWF overlap by introducing a suitable reduction factor ξ obtained by interpolating between the limiting cases of fully overlapping and nonoverlapping MLWFs. In particular, since in the DFT/vdW-WF2 method the ith MLWF is approximated with a homogeneous charged sphere of radius S_i, then the overlap among neighboring MLWFs can be evaluated as the geometrical overlap among neighboring spheres.[36] By extending the approach to partial overlaps, we define the *free* volume of a set of MLWFs belonging to a given fragment (in practice, three-dimensional integrals are evaluated by numerical sums introducing a suitable mesh in real space) as

$$V_{\text{free}} = \int d\mathbf{r}\, w_{\text{free}}(\mathbf{r}) \simeq \Delta r \sum_l w_{\text{free}}(\mathbf{r}_l), \tag{4}$$

where $w_{\text{free}}(\mathbf{r}_l)$ is equal to 1 if $|\mathbf{r}_l - \mathbf{r}_i| < S_i$ for at least one of the fragment MLWFs and is 0 otherwise.

The corresponding *effective* volume is instead given by

$$V_{\text{eff}} = \int d\mathbf{r}\, w_{\text{eff}}(\mathbf{r}) \simeq \Delta r \sum_l w_{\text{eff}}(\mathbf{r}_l)\,, \tag{5}$$

where the new weighting function is defined as $w_{\text{eff}}(\mathbf{r}_l) = w_{\text{free}}(\mathbf{r}_l)\, n_w(\mathbf{r}_l)^{-1}$, with $n_w(\mathbf{r}_l)$ that is equal to the number of MLWFs contemporarily satisfying the relation $|\mathbf{r}_l - \mathbf{r}_i| < S_i$. Therefore the nonoverlapping portions of the spheres (in practice, the corresponding mesh points) will be associated to a weight factor 1, those belonging to two spheres to a $1/2$ factor, and, in general, those belonging to n spheres to a $1/n$ factor. The average ratio between the effective volume and the free volume ($V_{\text{eff}}/V_{\text{free}}$) is then assigned to the factor ξ, appearing in Eq. (6). We therefore arrive at the following expression for the C_6 coefficient:

$$C_6^{AB} = \frac{3}{2} \frac{\sqrt{Z_A Z_B}\xi_A S_A^3 \xi_B S_B^3 \gamma^{3/2}}{\left(\sqrt{Z_B \xi_A} S_A^{3/2} + \sqrt{Z_A \xi_B} S_B^{3/2}\right)}\,, \tag{6}$$

where $\xi_{A,B}$ represents the ratio between the effective and the free volume associated to the Ath and Bth MLWF. The need for a proper treatment of overlap effects has been also recently pointed out by Andrinopoulos *et al.*,[29] who, however, applied a correction only to very closely centered WFCs.

Finally, the vdW interaction energy is computed as

$$E_{\text{vdW}} = -\sum_{i<j} f(R_{ij}) \frac{C_6^{ij}}{R_{ij}^6}, \tag{7}$$

where $f(R_{ij})$ is a short-range damping function, which is introduced not only to avoid the unphysical divergence of the vdW correction at small fragment separations, but also to eliminate double countings of correlation effects (in fact, standard DFT approaches are able to describe short-range correlations); it is defined as

$$f(R_{ij}) = \frac{1}{1 + e^{-a(R_{ij}/R_s - 1)}}\,. \tag{8}$$

The parameter R_s represents the sum of the vdW radii $R_s = R_i^{\text{vdW}} + R_j^{\text{vdW}}$, with (by adopting the same criterion chosen above for the γ parameter)

$$R_i^{\text{vdW}} = R_H^{\text{vdW}} \frac{S_i}{\sqrt{3}}, \tag{9}$$

where R_H^{vdW} is the literature[39] (1.20 Å) vdW radius of the H atom and, following Grimme *et al.*,[40] $a \simeq 20$ (the results are almost independent on the particular value of this parameter). Although this damping function introduces a certain degree of empiricism in the method, we stress that a is the only *ad hoc* parameter present in our approach, while all the others are only determined by the basic information given by the MLWFs, namely, from first-principles calculations. The evaluation of the vdW correction as a post-standard DFT calculation, using the DFT electronic density distribution, represents an approximation because, in principle, a full self-consistent calculations should be performed; however, investigations[41] on different systems have shown that the effects due to the lack of self-consistency are negligible, especially in proximity of the equilibrium, lowest-energy configuration, and for well separated fragments: in fact, one does not expect that the rather weak and diffuse vdW interaction substantially changes the electronic charge distribution.

In order to get an appropriate inclusion of screening effects, three different schemes have been adopted, hereafter referred to as DFT/vdW-WF2s1, DFT/vdW-WF2s2, and DFT/vdW-WF2s3, respectively, which are described in the following sections.

A. DFT/vdW-WF2s1

This scheme is similar to that previously applied[31] to the original DFT/vdW-WF method (see description above), however, now the vdW C_6 coefficients are computed by considering not only the more localized d-like MLWFs (as in Ref. 31, of course in the case of the Al(111) substrate the d-like MLWFs are absent) but also the s- and p-like electrons (so that all the MLWFs are taken into account); this being now more justified because in the DFT/vdW-WF2 method (differently from the original DFT/vdW-WF) the effect of relatively delocalized MLWFs is made less relevant by the proper treatment of intrafragment overlap, as described above. Then the screening reduction effect is included by multiplying (as in Ref. 31) the C_6^{ij}/R_{ij}^6 contribution in Eq. (7) by a Thomas-Fermi factor: $f_{\text{TF}} = e^{-2(z_s - z_l)/r_{\text{TF}}}$ where r_{TF} is the Thomas-Fermi screening length relative to the electronic density of a uniform electron gas ("jellium model") equal to the average density of the s- and p-like electrons of the substrate, z_s is the average vertical position of the topmost metal atoms, and z_l is the vertical coordinate of the WFC belonging to the substrate ($l = i$ if it is the ith WFCs which belongs to the substrate, otherwise $l = j$); the above f_{TF} function is only applied if $z_l < z_s$, otherwise it is assumed that $f_{\text{TF}} = 1$ (no screening effect).

B. DFT/vdW-WF2s2

In this alternative scheme, the screening is taken into account by adopting the following, two-step strategy, aiming at separating the effects of the relatively localized d-like orbitals from those of the more delocalized s- and p-like orbitals. (i) First, we compute the vdW energy correction by only considering the more localized d-like MLWFs, with the C_6 coefficients screened by the same Thomas-Fermi factor adopted for DFT/vdW-WF2s1; then by fitting (as in Ref. 31)

the calculated binding energies, at different adparticle-surface distances, with the function: $A\,e^{-Bz} - C_3/(z-z_0)^3$, A, B, C_3, and z_0 being adjustable parameters, we get an estimate of the Thomas-Fermi screened $C_{3d\mathrm{TF}}$ coefficient (and also of the unscreened C_{3d} coefficient if the Thomas-Fermi reduction factor is omitted).

(ii) Then the final vdW energy [see Eq. (7)] is evaluated by using "rescaled" C_6 coefficients, defined as

$$C_{6r}^{ij} = C_6^{ij}\,\frac{(C_{3d\mathrm{TF}} + C_{3f})}{C_{3d}}\,, \tag{10}$$

where C_{3f} is the C_3 coefficient evaluated by assuming the free-electron approximation for the metal surface, that is usually a reasonable estimate for the more delocalized s- and p-like orbital contribution[42] and can be easily computed[2] as

$$C_{3f} = \frac{\alpha_0}{8}\hbar\frac{\omega_0\omega_p}{\omega_0+\omega_p}\,, \tag{11}$$

where α_0 and ω_0 are the static polarizability and the characteristic frequency of the adsorbed adparticle, respectively, and ω_p is the plasma frequency of the metal substrate (appropriate to the electron density relative to s and p electrons). α_0 and ω_p values can be easily found in the literature, and ω_0 can be expressed[43] in terms of α_0:

$$\omega_0 = \sqrt{\frac{Ze^2}{m\alpha_0}}\,, \tag{12}$$

where Z is the number of valence electrons of the adparticle and e and m are the electronic charge and mass, respectively. In the fitting function $A\,e^{-Bz} - C_3/(z-z_0)^3$, the image-plane position z_0 can be taken[32] as half the interlayer distance of the substrate (in fact, half a normal lattice spacing above the outermost layer of substrate nuclei can be taken as the jellium-edge position[44]) and z is the distance of the adsorbed adparticle from the surface.

In the case of H_2 on Al(111), d-like orbitals are absent and Eq. (10) reduces to

$$C_{6r}^{ij} = C_6^{ij}\,\frac{C_{3f}}{C_3}\,, \tag{13}$$

where C_3 is the unscreened C_3 coefficient, always obtained by fitting the $A\,e^{-Bz} - C_3/(z-z_0)^3$ function.

This second scheme, DFT/vdW-WF2s2, based on rescaled C_6 coefficients, follows a strategy similar to that adopted in Ref. 32, where screening effects are included in the TS-vdW method[45] by using the Lifshitz-Zaremba-Kohn theory[46] for the vdW interaction between an atom and a solid surface, which describes the many-body collective response of the substrate electrons.

C. DFT/vdW-WF2s3

A simple approach to mimic screening effects in adsorption processes is represented by the so-called "single-layer" approximation in which vdW effects are only restricted to the interactions of the adparticle with the topmost metal layer;[47] in fact, as a consequence of screening, one expects that the topmost metal atoms give the dominant contribution. We have implemented this by multiplying the C_6^{ij}/R_{ij}^6 factor in Eq. (7) by a damping function:

$$f_{\mathrm{SL}} = 1 - \frac{1}{1+e^{(z_l-z_r)/\Delta z}}\,, \tag{14}$$

where z_l is the vertical coordinate of the WFC belonging to substrate ($l=i$ if it is the ith WFCs, which belongs to the substrate, otherwise $l=j$), the reference level z_r is taken as intermediate between the level of the first, topmost surface layer and the second one, and we assume that Δz = (interlayer separation)/4; we found that the estimated equilibrium binding energies and adparticle-surface distances exhibit only a mild dependence on the Δz parameter. Clearly, this third approach resembles the DFT/vdW-WF2s1 scheme, the basic difference being that the Thomas-Fermi damping function of DFT/vdW-WF2s1 is here replaced by the f_{SL} damping function introduced to just select the WFCs around the topmost surface layer. Although f_{SL} is, in principle, less physically motivated than the Thomas-Fermi function, its practical effect is expected to be very similar, as confirmed by the applications of the methods (see Results).

D. Computational details

We here apply the DFT/vdW-WF2s1, DFT/vdW-WF2s2, and DFT/vdW-WF2s3 methods to the case of adsorption of RGs, H_2, CH_4, and H_2O on the Cu(111) surface and of H_2 on Al(111) and Xe on Pb(111). All calculations have been performed with the QUANTUM ESPRESSO *ab initio* package[48] (MLWFs have been generated as a postprocessing calculation using the WANT package[49]). Similarly to our previous study,[31] we modeled the metal surface using a periodically repeated hexagonal supercell, with a $(\sqrt{3}\times\sqrt{3})R30^\circ$ structure and a surface slab made of 15 Cu, Al, or Pb atoms distributed over five layers (repeated slabs were separated along the direction orthogonal to the surface by a vacuum region of about 24 Å). The Brillouin zone has been sampled using a $6\times6\times1$ k-point mesh. In this model system, the coverage is 1/3, i.e., one adsorbed adparticle for each three metal atoms in the topmost surface layer. The $(\sqrt{3}\times\sqrt{3})R30^\circ$ structure has been indeed observed[4] at low temperature by LEED for the case of Xe adsorption on Cu(111) and Pd(111) (actually, this is the simplest commensurate structure for RG monolayers on close-packed metal surfaces and the only one for which good experimental data exist), and it was adopted in most of the previous *ab initio* studies.[7–9,11,12,50] The metal surface atoms were kept frozen (of course, after a preliminary relaxation of the outermost layers of the clean metal surfaces) and only the vertical coordinate (perpendicular to the surface) of the center of mass of the adparticles was optimized, this procedure being justified by the fact that only minor surface atom displacements are observed upon physisorption.[8,50–52] Moreover, the adparticles were adsorbed on both sides of the slab: in this way, the surface dipole generated by adsorption on the upper surface of the slab is canceled by the dipole appearing on the lower surface, thus greatly reducing the spurious dipole-dipole interactions between the periodically repeated images (previous DFT-based calculations have shown that these choices are appropriate[9,13,18,31]).

We have carried out calculations for various separations of the atoms and molecules adsorbed on the *top* high-symmetry

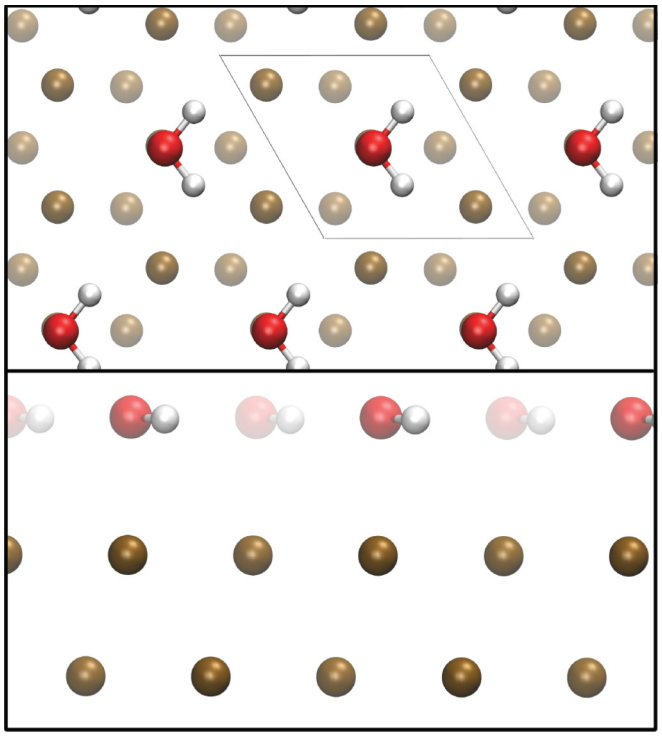

FIG. 1. (Color online) Plan (top) and side (bottom) views for a single water molecule on the Cu(111) surface, showing the simulation cell and the periodic images.

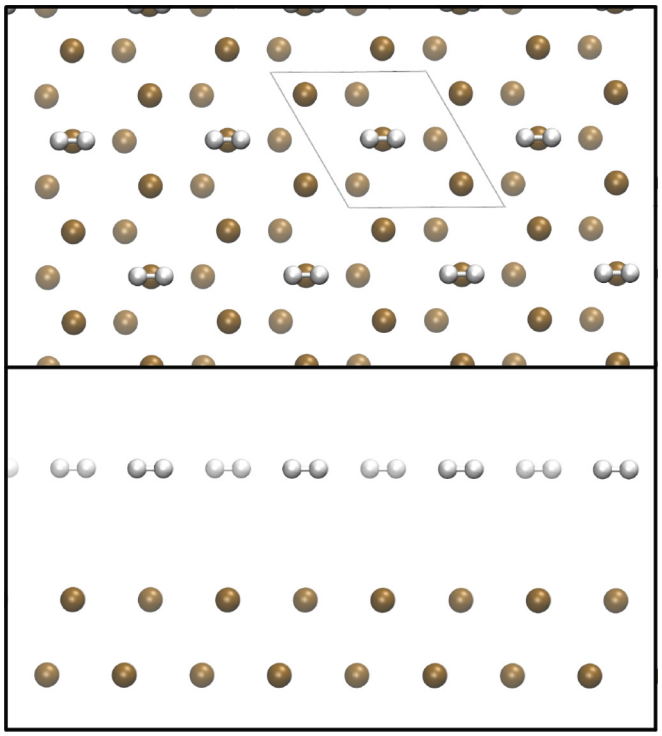

FIG. 2. (Color online) Plan (top) and side (bottom) views for a single hydrogen molecule on the Cu(111) surface, showing the simulation cell and the periodic images.

site (on the top of a metal atom), since this is certainly the favored adsorption site for Xe on Cu(111);[31] in the case of H_2, CH_4, and H_2O by adsorption on the top site we mean that the center of mass of these molecules is on top of a Cu atom (see Figs. 1 and 2), which is assumed to be the preferred adsorption site.[17,19,21,53] For the Xe-Cu(111) and Xe-Pb(111) cases, we have also considered adsorption on the *hollow* site (on the center of the triangle formed by the three surface metal atoms contained in the supercell) in order to verify whether the present schemes are able to correctly predict which configuration is energetically favored (see discussion in Ref. 31). In the calculations, the H_2 molecule is kept in a flat orientation above the Cu(111) surface (the binding energy depends very little on the orientation[17,54]). The same is true for the water monomer since there is a general agreement[19] that the water molecule prefers to bind in a top position on the Cu(111) substrate, with its molecular plane nearly parallel to the surface.

For a better accuracy, as done in previous applications on adsorption processes,[28,31,35,55,56] we have also included the interactions of the MLWFs of the physisorbed fragments not only with the MLWFs of the underlying surface, within the reference supercell, but also with a sufficient number of periodically-repeated surface MLWFs (in any case, given the R^{-6} decay of the vdW interactions, the convergence with the number of repeated images is rapidly achieved). Electron-ion interactions were described using norm-conserving pseudopotentials by explicitly including 14, 11, and 3 valence electrons per Pb, Cu, and Al atom, respectively. As in our previous study,[31] we chose the PW91[57] reference DFT functional. The problem of choosing the optimal DFT functional, particularly in its exchange component, to be combined with long-range vdW interactions and the related problem of completely eliminating double counting of correlation effects [which, in our scheme, is accomplished by the short-range damping function $f(R_{ij})$ defined above] still remain open;[24] however, they are expected to be more crucial for adsorption systems characterized by relatively strong adparticle-substrate bonds ("chemisorption") and, for instance, for the determination of the perpendicular vibration frequency[11] than for the equilibrium properties of the physisorbed systems, we focus on in our paper.

The additional cost of the post-processing vdW correction is basically represented by the cost of generating the maximally localized Wannier functions from the Kohn-Sham orbitals, which scales linearly with the size of the system.[30] In our specific applications, the Wannier-function generation is more expensive because of the k-point sampling of the Brillouin zone, that is appropriate for metals and make the spread-minimization process less efficient.[30] In practice, in our cases, the additional cost of the vdW correction is comparable with that of the previous standard DFT calculation, however, one must point out that, for generating the maximally localized Wannier functions, we have just used the public-released scalar version of the WANT code[49] without any attempt to develop a much faster parallelized version or to make the minimization process more efficient.

III. RESULTS AND DISCUSSION

In Tables I– VIII results are reported for all the systems under consideration; in particular, in Tables I, V, and VII, we

TABLE I. Binding energy, E_b in meV, of adparticles in the top configuration on the metal surface computed using the standard PW91 calculation, and including the vdW corrections using our (unscreened) DFT/vdW-WF2, and (screened) DFT/vdW-WF2s1, DFT/vdW-WF2s2, and DFT/vdW-WF2s3 methods.

System	PW91	DFT/vdW-WF2	DFT/vdW-WF2s1	DFT/vdW-WF2s2	DFT/vdW-WF2s3
H_2-Cu(111)	−10.5	−49.8	−36.0	−25.6	−33.7
H_2-Al(111)	−14.7	−35.2	−22.9	−25.9	−26.5
Ne-Cu(111)	−17.5	−66.3	−50.8	−34.9	−52.2
Ar-Cu(111)	−13.0	−140.1	−91.3	−66.4	−97.8
Kr-Cu(111)	−20.3	−196.8	−130.5	−102.2	−131.3
Xe-Cu(111)	−23.1	−333.2	−214.5	−242.7	−224.2
Xe-Pb(111)	−56.3	−151.9	−100.0	−210.0	−111.9
CH_4-Cu(111)	−16.1	−166.1	−111.9	−119.5	−112.7
H_2O-Cu(111)	−71.0	−425.4	−345.7	−350.1	−345.3

compare quantities evaluated by the standard PW91 approach, and including the vdW corrections using our (unscreened) DFT/vdW-WF2 method, and the screened schemes DFT/vdW-WF2s1, DFT/vdW-WF2s2, and DFT/vdW-WF2s3 described above; in Tables II–IV, VI, and VIII we instead compare our global, screened DFT/vdW-WF2s estimates (obtained by considering the range of values calculated separately by the DFT/vdW-WF2s1, DFT/vdW-WF2s2, and DFT/vdW-WF2s3 methods), to available theoretical and experimental estimates and to corresponding data obtained using the "seamless" vdW-DF and vdW-DF2 methods of Langreth *et al.*,[41,58,59] which perform well in a variety of applications, although they are not perfect since they violate some important limits;[60] moreover, they do not explicitly take into account screening effects of metal surfaces.[17]

The *binding energy* E_b is defined as

$$E_b = 1/2[E_{\rm tot} - (E_s + 2E_a)], \tag{15}$$

where $E_{s,a}$ represent the energies of the isolated fragments (the substrate and the adparticles) and $E_{\rm tot}$ is the energy of the interacting system, including the vdW-correction term (the factors 2 and 1/2 are due to the adsorption on both sides of the slab); E_s and E_a are evaluated using the same supercell adopted for $E_{\rm tot}$.

The experimentally measured *adsorption energy* E_a often includes not only the interaction of adparticles with the substrate but also lateral vdW interfragment interactions.[13,31] Therefore sometimes it is more appropriate to compare experimental data with the quantity E_a, which can be related to E_b by[31]

$$E_a = E_b + (E_l - E_f)\,, \tag{16}$$

where E_l is the total energy (per particle) of the 2D lattice formed by the adparticles only (that is as in the adsorption configurations but without the substrate and including vdW

TABLE II. Binding energy, E_b in meV, of adparticles in the top configuration on the metal surface computed considering our DFT/vdW-WF2s estimates (within the range of values obtained by the DFT/vdW-WF2s1, DFT/vdW-WF2s2, and DFT/vdW-WF2s3 methods), compared to the vdW-DF and the vdW-DF2 methods by Langreth *et al.*[41,58,59] and available theoretical and experimental (in parenthesis) reference data.

System	DFT/vdW-WF2s	vdW-DF	vdW-DF2	Reference
H_2-Cu(111)	−36↔ −26	−53	−39	−32[a] (−29[b])
H_2-Al(111)	−27↔ −23	−59	−47	−19[c] −24[d] (−37[e])
Ne-Cu(111)	−52↔ −35	−56	−37	···
Ar-Cu(111)	−98↔ −66	−106	−91	−85[a]
Kr-Cu(111)	−131↔ −102	−136	−116	−119[a]
Xe-Cu(111)	−243↔ −214	−168	−156	−280[f], −183[a], −277[g], −270[h] (−190[g],−227[i])
Xe-Pb(111)	−210↔ −100	−186	−136	···
CH_4-Cu(111)	−119↔ −112	−124	−108	···
H_2O-Cu(111)	−350↔ −345	−133	−141	···

[a]Reference 2.
[b]Reference 17.
[c]Reference 62.
[d]Reference 54.
[e]Reference 61.
[f]Reference 11.
[g]Reference 4.
[h]Reference 14.
[i]Reference 76.

TABLE III. Adsorption energy, E_a in meV (see text for the definition), of methane and water in the top configuration on the Cu(111) surface computed considering our DFT/vdW-WF2s estimates (within the range of values obtained by the DFT/vdW-WF2s1, DFT/vdW-WF2s2, and DFT/vdW-WF2s3 methods), compared to the vdW-DF and the vdW-DF2 methods by Langreth *et al.*[41,58,59] and available experimental reference data.

System	DFT/vdW-WF2s	vdW-DF	vdW-DF2	Reference
CH_4-Cu(111)	$-185 \leftrightarrow -178$	-205	-166	-160[a]
H_2O-Cu(111)	$-446 \leftrightarrow -441$	-240	-223	-352[b]

[a]Reference 65.
[b]Reference 73.

interfragment corrections when vdW-corrected methods are used) and E_f is the energy of an isolated (free) adparticle.

E_b has been evaluated for several adsorbate-substrate distances; then the equilibrium distances and the corresponding binding energies have been obtained (as in Ref. 31, see also the Method section) by fitting the calculated points with the function: $A\,e^{-Bz} - C_3/(z - z_0)^3$ [as illustrated for the H_2-Cu(111) case in Fig. 3]. Typical uncertainties in the fit are of the order of 0.05 Å for the distances and a few meVs for the minimum binding energies. When vdW interactions dominate, the equilibrium binding energy is expected to be roughly proportional to the adparticle polarizabilities.[44] As found in the previous studies[31] (see Fig. 3 and Tables I and V), the effect of the vdW-corrected schemes is a much stronger bonding than with a pure PW91 scheme, with the formation of a clear minimum in the binding energy curve at a shorter equilibrium distance. Moreover, by comparing with unscreened data (we recall that also the vdW-DF and vdW-DF2 methods do not take explicitly metallic screening into account), we see that the effect of screening is substantial, leading to reduced binding energies and increased adparticle-substrate equilibrium distances.

By first considering the adsorption of H_2 on Cu(111) for which accurate reference data are available, both the experimental binding energy (-29 meV) and the equilibrium H_2-Cu(111) distance ($z_{eq} = 3.52$ Å) are well reproduced (see Tables I, II, V and VI, and Fig. 3) by our screened methods (with DFT/vdW-WF2s1 and DFT/vdW-WF2s3 that slightly overestimate the strength of the interaction and DFT/vdW-WF2s2 that slightly underestimates it, the trend being reversed for the equilibrium distance). Interestingly, our results are much better than those obtained by the vdW-DF[41,58] ($E_b = -53$ meV, $z_{eq} = 3.85$ Å), DFT-D3[40] ($E_b = -98$ meV, $z_{eq} = 2.86$ Å), and TS-vdW[45] ($E_b = -66$ meV, $z_{eq} = 3.20$ Å) methods, and also slightly better than the estimates of vdW-DF2[59] ($E_b = -39$ meV, $z_{eq} = 3.64$ Å). We therefore confirm the observations of Lee *et al.* who, by comparison with the reference potential energy curve of H_2 on Cu(111), concluded that vdW-DF2 performs relatively well (the remaining discrepancy being probably due to lack of screening-effect description[17]), differently from DFT-D3 and TS-vdW, a behavior attributed to the fact that pair potentials, on which these two methods are based, center the interactions on the nuclei and do not fully reflect that important binding contributions arise in the wave function tails outside the surface.[17] Concerning the C_3 coefficients (see Tables VII and VIII), these represent notorious difficult quantities to evaluate (see, for instance, Refs. 1 and 31): in fact, the reliability of reference data is hard to assess, moreover, one should really make estimates by sampling the asymptotic region, corresponding to large adparticle-surface distances, where the binding energy is quite small and the relative uncertainty large. Moreover, for characterizing the adsorption processes, the focus is mainly on the equilibrium properties, corresponding to a region not far from the minimum of the adparticle-surface binding-energy curve. In any case, for the C_3 coefficient of H_2 on Cu(111), the agreement with the reference data is less satisfactory than for E_b and z_{eq}, and comparable with that of vdW-DF2, while instead vdW-DF clearly strongly overestimates. Note that, by using the simple DFT/vdW-WF2s3 approach, for this system one gets results comparable (see Fig. 3) with those obtained by DFT/vdW-WF2s1 and DFT/vdW-WF2s2 with the C_3 coefficient that is even closer to the reference value.

TABLE IV. Difference, ΔE_b, in meV, between the binding energy E_b of Xe on metal surfaces in the *top* and *hollow* configurations, computed considering our DFT/vdW-WF2s estimates (within the range of values obtained by the DFT/vdW-WF2s1, DFT/vdW-WF2s2, and DFT/vdW-WF2s3 methods), compared to the vdW-DF and the vdW-DF2 methods by Langreth *et al.*[41,58,59]

System	DFT/vdW-WF2s	vdW-DF	vdW-DF2
Xe-Cu(111)	$-40 \leftrightarrow -37$	-3	-1
Xe-Pb(111)	$+8 \leftrightarrow +22$	$+6$	$+3$

If H_2 is instead adsorbed on the Al(111) surface, accurate reference data are more scarce: there is just an indirect experimental estimate[61] for E_b (-37 meV), old theoretical calculations based on jellium models[62,63] or damped dipole-dipole and dipole-quadrupole interactions,[54] and a study performed using a density functional for asymptotic vdW forces.[64] By considering the reference binding energies one can see that, also in this case, the performances of the DFT/vdW-WF2s1, DFT/vdW-WF2s2, and DFT/vdW-WF2s3 methods are satisfactory and comparable: all the methods predict (see Table II) values slightly below the experimental estimate, the agreement being better with previous theoretical calculations, while vdW-DF and vdW-DF2 tend to overestimate the strength of the interaction (again vdW-DF2 performs better than vdW-DF). The experimental estimate of the equilibrium distance appears instead significantly smaller than the values obtained by all the theoretical methods considered in the present study. For the C_3 coefficients, the same observations relative to the H_2-Cu(111) case apply.

Considering the adsorption of RGs on Cu(111), reference data are available, particularly the "best estimates" reported by Vidali *et al.*,[2] that represent averages over different theoretical and experimental evaluations. As can be seen, for Ne, Ar, and Kr on Cu(111) the DFT/vdW-WF2s1, DFT/vdW-WF2s2, and DFT/vdW-WF2s3 methods give binding energies compatible with those obtained by vdW-DF2, while vdW-DF tends instead to overbind: this is also confirmed by the fact that vdW-DF predicts C_3 values much larger than the other schemes and comparable to those obtained by our DFT/vdW-WF2 method without any screening correction. Note that, as a general

TABLE V. Equilibrium adparticle-metal surface distance, in angstroms, of adparticles in the top configuration computed using the standard PW91 calculation, and including the vdW corrections using our (unscreened) DFT/vdW-WF2, and (screened) DFT/vdW-WF2s1, DFT/vdW-WF2s2, and DFT/vdW-WF2s3 methods.

System	PW91	DFT/vdW-WF2	DFT/vdW-WF2s1	DFT/vdW-WF2s2	DFT/vdW-WF2s3
H_2-Cu(111)	4.10	3.24	3.40	3.60	3.49
H_2-Al(111)	4.08	3.84	3.93	3.92	3.91
Ne-Cu(111)	3.90	3.38	3.44	3.56	3.43
Ar-Cu(111)	4.50	3.26	3.41	3.54	3.39
Kr-Cu(111)	4.50	3.05	3.36	3.38	3.37
Xe-Cu(111)	4.40	2.97	3.12	3.04	3.15
Xe-Pb(111)	4.50	3.98	4.07	3.73	4.06
CH_4-Cu(111)	4.70	3.39	3.49	3.43	3.52
H_2O-Cu(111)	2.81	2.40	2.41	2.36	2.43

trend, both vdW-DF and vdW-DF2 give larger equilibrium distances than our DFT/vdW-WF2s1, DFT/vdW-WF2s2, and DFT/vdW-WF2s3 methods. For Xe-Cu(111), the scenario appears to be more complex: in fact, with respect to the reference values, our screened methods appear to well reproduce the equilibrium binding energy and C_3 coefficient, although the equilibrium distances are shorter; instead vdW-DF and vdW-DF2 overestimate the equilibrium Xe-Cu(111) distance and the C_3 coefficient, while they undererestimate the binding energies. This peculiar behavior can be probably explained by the tendency of Xe to induce a substantial electronic charge delocalization on the Cu(111) surface,[31] thus making screening effects relatively less important than for the other RGs. Probably in this case the results also depend in a more subtle way on the specific choice of the underlying DFT functional. Interestingly, all the considered theoretical schemes (see Table IV) predict that the top site is favored with respect to the hollow one for Xe on Cu(111) (in agreement with the experimental evidence[6]), while the opposite is true for Xe on Pb(111) (in line with previous calculations[31]), although vdW-DF and vdW-DF2 clearly tend to minimize the differences.

Concerning the case of methane on Cu(111), the experimental adsorption energy has been estimated by temperature-programmed-desorption measurements of the activation energy (160 meV) for molecular desorption of methane from a saturated first monolayer,[65] so that it includes the lateral interactions mentioned above and it is more appropriate to compare this estimate with the E_a quantity defined in Eq. (16). As can be seen in Table III the performances of the different schemes exhibit the same trend observed in the previous investigated cases: DFT/vdW-WF2s1, DFT/vdW-WF2s2, DFT/vdW-WF2s3, and vdW-DF2 gives similar adsorption energies (with vdW-DF2 that in this case is closer to the reference value), while vdW-DF appears to overbind; the C-Cu(111) equilibrium distance and the C_3 coefficient are larger with vdW-DF and vdW-DF2 than with DFT/vdW-WF2s1, DFT/vdW-WF2s2, and DFT/vdW-WF2s3.

Coming to our final system, namely the water monomer on Cu(111), in this case the experimental characterization is made

TABLE VI. Equilibrium adparticle-metal surface distance, in angstroms, of adparticles in the top configuration computed considering our DFT/vdW-WF2s estimates (within the range of values obtained by the DFT/vdW-WF2s1, DFT/vdW-WF2s2, and DFT/vdW-WF2s3 methods), compared to the vdW-DF and the vdW-DF2 methods by Langreth *et al.*[41,58,59] and available theoretical and experimental (in parenthesis) reference data.

System	DFT/vdW-WF2s	vdW-DF	vdW-DF2	Reference
H_2-Cu(111)	3.40↔3.60	3.85	3.64	2.86[a], 3.2[a] (3.52[a])
H_2-Al(111)	3.91↔3.93	3.94	3.75	3.52[b]
Ne-Cu(111)	3.43↔3.56	3.68	3.68	...
Ar-Cu(111)	3.39↔3.54	3.86	3.74	3.53[c]
Kr-Cu(111)	3.36↔3.38	3.99	3.75	...
Xe-Cu(111)	3.04↔3.15	4.09	3.93	3.2↔4.0[d] (3.6[e])
Xe-Pb(111)	3.73↔4.07	4.30	4.29	...
CH_4-Cu(111)	3.43↔3.52	4.14	3.99	...
H_2O-Cu(111)	2.36↔2.43	3.27	3.05	2.25[f], 2.36[g]

[a]Reference 17.
[b]Reference 54.
[c]Reference 77.
[d]Reference 31.
[e]Reference 4.
[f]Reference 21.
[g]Reference 78.

TABLE VII. Estimated C_3 coefficients, in meVÅ^3, for adparticles in the top configuration on the metal surface computed using our (unscreened) DFT/vdW-WF2, and (screened) DFT/vdW-WF2s1, DFT/vdW-WF2s2, and DFT/vdW-WF2s3 methods.

System	DFT/vdW-WF2	DFT/vdW-WF2s1	DFT/vdW-WF2s2	DFT/vdW-WF2s3
H_2-Cu(111)	1485	1171	984	1216
H_2-Al(111)	1442	943	1098	1103
Ne-Cu(111)	1698	1443	1018	1415
Ar-Cu(111)	3078	2277	2030	2235
Kr-Cu(111)	5036	3593	2848	3858
Xe-Cu(111)	5601	4016	3480	3995
Xe-Pb(111)	4242	2935	4263	3317
CH_4-Cu(111)	3533	2559	2523	2720
H_2O-Cu(111)	2386	1892	1612	1986

difficult by facile water-cluster formation that masks the true H_2O-metal interaction.[20] In any case, previous studies indicate that it is easier to desorb than to dissociate H_2O on the Cu(111) and Cu(110) surfaces (see Ref. 66 and references therein). The system has been already studied using pure GGA (mainly based on PW91 and PBE functionals) or hybrid (B3LYP) approaches,[19,21,52,66–71] giving rather spread estimates for the binding energy (between −120 and −660 meV) and the Cu-O equilibrium distance (between 2.2 and 3.9 Å), these relatively large differences being mainly attributed to the different exchange-correlation functionals adopted (besides other technical details, including surface coverage, reference supercell, geometry optimization conditions, number of considered Cu planes, pseudopotentials, plane-wave energy cutoff, etc.). In all these studies, a proper description of vdW effects is missing. Higher-level (MP2) *ab initio* calculations exist,[72] that should include vdW interactions, predicting that the energetically favored adsorption configuration is characterized by an H-down conformation (with a binding energy of −166 meV and an equilibrium Cu-O distance of 3.59 Å), differently from the other studies which instead predict an almost planar equilibrium configuration for the water monomer on the Cu surface; however, these results are questionable since the Cu(111) surface is modeled by relatively small Cu clusters, which are affected by well-known size-dependent effects. The energy values of the H_2O-Cu(111) bond indicate that it lies in the weak chemisorption/physisorption regime;[21] interestingly, this energy range (about 0.25 eV) also represents the energy of a typical H-bond between water molecules,[20] so that adsorbate-adsorbate and adsorbate-substrate interactions are comparable. Old experimental estimates for water on Cu(111) are available,[20] however, these values (in the range from −0.4 to −0.7 eV) are probably overestimated[52] since they possibly correspond to polycrystalline samples containing a large number of low-coordinated surface atoms. An estimate[73] for the adsorption energy of water on Cu(111), on the basis of x-ray photoelectron spectroscopy, gives −352 meV. Although it is believed[74] that vdW effects are not crucial for many aspects of structure and bonding of H_2O on Cu(111), nonetheless, due to the high polarizability of the substrate metal atoms,

TABLE VIII. Estimated C_3 coefficients, in meVÅ^3, for adparticles in the top configuration on the metal surface computed using our DFT/vdW-WF2s data (within the range of values obtained by the DFT/vdW-WF2s1, DFT/vdW-WF2s2, and DFT/vdW-WF2s3 methods), compared to the vdW-DF and the vdW-DF2 methods by Langreth *et al.*[41,58,59] and available theoretical reference data.

System	DFT/vdW-WF2s	vdW-DF	vdW-DF2	Reference
H_2-Cu(111)	984↔1216	2310	1097	681[a], 673[b]
H_2-Al(111)	943↔1103	2427	1279	605[c], 661[d], 669[e], 706[f]
Ne-Cu(111)	1018↔1443	1644	801	488[a], 417[g]
Ar-Cu(111)	2030↔2277	4690	2641	1621[b], 1397[g]
Kr-Cu(111)	2848↔3858	6722	3962	2294[a], 2110[b], 1992[g]
Xe-Cu(111)	3480↔4016	9712	6146	3391[a], 3390[b], 2967[g]
Xe-Pb(111)	2935↔4263	8837	5506	. . .
CH_4-Cu(111)	2523↔2720	6735	3967	. . .
H_2O-Cu(111)	1612↔1986	4167	2297	. . .

[a]Reference 79.
[b]Reference 2.
[c]Reference 64.
[d]Reference 62.
[e]Reference 54.
[f]Reference 63.
[g]Reference 80.

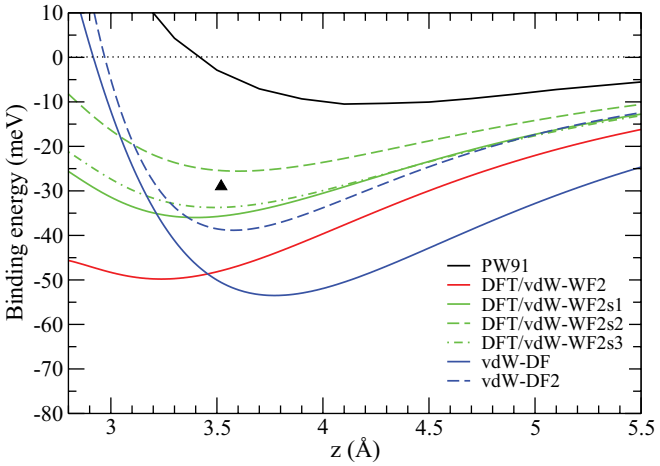

FIG. 3. (Color online) Binding energy of H_2 on Cu(111), as a function of the distance between the center of mass of H_2 and the Cu(111) surface, computed using the standard PW91 calculation and including the vdW corrections using our (unscreened) DFT/vdW-WF2, and (screened) DFT/vdW-WF2s1, DFT/vdW-WF2s2, and DFT/vdW-WF2s3 methods, and the vdW-DF and the vdW-DF2 methods by Langreth *et al.*;[41,58,59] the triangle indicates the position of the experimental value.

they contribute substantially to the water-metal bond, which is an important factor in determining the relative stabilities of wetting layers and 3D bulk ice.[74]

In our study, for the sake of uniformity, we have maintained the $(\sqrt{3} \times \sqrt{3})R30^\circ$ supercell also for H_2O on Cu(111), although the 2×2 simulation cell would be, in principle, more appropriate in this case (with the smaller $(\sqrt{3} \times \sqrt{3})R30^\circ$ cell the separation between the periodic images of the water molecule is smaller and the coverage is higher than with the 2×2 supercell, which may lead to stronger adsorbate-adsorbate interactions that affect the adsorption[70]). Using this supercell, we have explicitly verified that the quasi-planar structure is the favored one for the water monomer on Cu(111).

As can be seen in Table III, again DFT/vdW-WF2s1, DFT/vdW-WF2s2, and DFT/vdW-WF2s3 give similar results, while vdW-DF and vdW-DF2 predict lower adsorption energies and larger O-Cu(111) equilibrium distances and C_3 coefficients. Note that, concerning the equilibrium distance, whose reference values are restricted within a relatively narrow range, DFT/vdW-WF2s1, DFT/vdW-WF2s2, and DFT/vdW-WF2s3 perform much better than vdW-DF and vdW-DF2. As expected, in this case a pure (i.e. non vdW-corrected) PW91 calculation gives already a significant amount of the binding energy (about 20% considering DFT/vdW-WF2s1, DFT/vdW-WF2s2 and DFT/vdW-WF2s3, see Table I) and the screening corrections are relatively less relevant than in the previous systems where the vdW interactions were dominant. In fact, although the water molecule and, for instance, the Ar atom have the same number (8) of valence electrons and similar polarizabilities, electrostatic effects are also of importance for water due to its intrinsic electronic dipole moment.

In the present study we focus on (111) surfaces only, although our approach is expected to be applicable to other, interesting substrates, as already shown in preliminary applications of the original DFT/vdW-WF scheme on the interaction of Ar, He, and H_2 with two different Al surfaces.[28] Changing the surface face can have different effects on adsorption processes. For instance, in the case of H_2 on copper the experimental-based and computed potential-energy curves of physisorption of H_2 on the Cu(111), Cu(100), and Cu(110) surfaces are very similar;[17] for H_2 on aluminum, the measured physisorption well depth is similar for the (111) and (110) faces of Al but larger than for the intermediate (100) face.[61] For water on copper, the interaction is stronger with the open Cu(110) and Cu(100) surfaces than with the more closely packed Cu(111) surface.[70]

IV. CONCLUSIONS

In summary, we have investigated the adsorption of RGs and small molecules, H_2, CH_4, and H_2O on the Cu(111) metal surface, and of H_2 on Al(111), and Xe on Pb(111), by considering three different recipes to include screening effects in our recently developed DFT/vdW-WF2 method. By analyzing the results of our study and comparing them to available reference data, we get a substantial improvement with respect to the original, unscreened approach. Given the uncertainties in the reference data, one cannot easily state which scheme is more appropriate. Considering all the studied cases and, in particular, H_2-Cu(111) for which more reliable reference data are available, DFT/vdW-WF2s2 turns out to be marginally superior which correlates with the relatively higher complexity of this approach. Interestingly, we confirm the conclusion of previous studies (see, Ref. 47 and references therein) which suggest that, particularly for the close-packed (111) surfaces, the assumption of a one-layer screening depth (single-layer approximation) works reasonably well. The differences between the values of the equilibrium binding energies and distances predicted by the three different schemes can be taken as the order of magnitude of the uncertainty associated to the screened DFT/vdW-WF2 method and to estimate its accuracy. Looking at the results reported in the tables, it turns out that these differences are relatively large for the case of Xe on Pb(111), essentially because the DFT/vdW-WF2s2 schemes predict a stronger bonding than DFT/vdW-WF2s1 and DFT/vdW-WF2s3. This behavior is probably due to the fact that the free-electron approximation for the *s*- and *p*-like orbital contribution, on which the DFT/vdW-WF2s2 approach is based [see Eq. (10)], is less appropriate for Pb than for a noble metal like Cu or for Al.

For the considered systems, in general our methods perform better than the popular (unscreened) vdW-DF and vdW-DF2 approaches, which, in particular, exhibit a general tendency to overestimate the equilibrium distances, in line with the behavior reported for systems including a metallic surface.[75] We also suggest that the vdW-DF2 method should be preferred to vdW-DF for this kind of applications.

ACKNOWLEDGMENT

We thank very much Flavio Toigo for useful discussions.

*Present Address: Fritz Haber Institut der Max Planck Gesellschaft, Faradayweg 4-6, 14195, Berlin, Germany.

[1] L. W. Bruch, M. W. Cole, and E. Zaremba, *Physical Adsorption: Forces and Phenomena* (Clarendon Press, Oxford, 1997).

[2] G. Vidali, G. Ihm, H. Y. Kim, and M. W. Cole, Surf. Sci. Rep. **12**, 133 (1991).

[3] J. M. Gottlieb, Phys. Rev. B **42**, 5377 (1990).

[4] Th. Seyller, M. Caragiu, R. D. Diehl, P. Kaukasoina, and M. Lindroos, Chem. Phys. Lett. **291**, 567 (1998); M. Caragiu, Th. Seyller, and R. D. Diehl, Phys. Rev. B **66**, 195411 (2002).

[5] B. Narloch and D. Menzel, Chem. Phys. Lett. **290**, 163 (1997).

[6] R. D. Diehl, Th. Seyller, M. Caragiu, G. S. Leatherman, N. Ferralis, K. Pussi, P. Kaukasoina, and M. Lindroos, J. Phys.: Condens. Matter **16**, S2839 (2004).

[7] J. L. F. Da Silva, C. Stampfl, and M. Scheffler, Phys. Rev. Lett. **90**, 066104 (2003).

[8] J. L. F. Da Silva, C. Stampfl, and M. Scheffler, Phys. Rev. B **72**, 075424 (2005).

[9] J. L. F. Da Silva and C. Stampfl, Phys. Rev. B **77**, 045401 (2008).

[10] A. E. Betancourt and D. M. Bird, J. Phys.: Condens. Matter **12**, 7077 (2000).

[11] P. Lazić, Ž. Crljen, R. Brako, and B. Gumhalter, Phys. Rev. B **72**, 245407 (2005).

[12] M. C. Righi and M. Ferrario, J. Phys.: Condens. Matter **19**, 305008 (2007).

[13] X. Sun and Y. Yamauchi, J. Appl. Phys. **110**, 103701 (2011).

[14] D.-L. Chen, W. A. Al-Saidi, and J. K. Johnson, Phys. Rev. B **84**, 241405(R) (2011).

[15] D.-L. Chen, W. A. Al-Saidi, and J. K. Johnson, J. Phys.: Condens. Matter **24**, 424211 (2012).

[16] P. S. Bagus, V. Staemmler, and C. Wöll, Phys. Rev. Lett. **89**, 096104 (2002).

[17] K. Lee, A. K. Kelkkanen, K. Berland, S. Andersson, D. C. Langreth, E. Schröder, B. I. Lundqvist, and P. Hyldgaard, Phys. Rev. B **84**, 193408 (2011); K. Lee, K. Berland, M. Yoon, S. Andersson, E. Schröder, P. Hyldgaard, and B. I. Lundqvist, J. Phys.: Condens. Matter **24**, 424213 (2012).

[18] T. S. Chwee and M. B. Sullivan, J. Chem. Phys. **137**, 134703 (2012).

[19] A. Hodgson and S. Haq, Surf. Sci. Rep. **64**, 381 (2009).

[20] P. A. Thiel and T. E. Madey, Surf. Sci. Rep. **7**, 211 (1987).

[21] A. Michaelides, V. A. Ranea, P. L. de Andres, and D. A. King, Phys. Rev. Lett. **90**, 216102 (2003).

[22] See, for instance, W. Kohn, Y. Meir, and D. E. Makarov, Phys. Rev. Lett. **80**, 4153 (1998).

[23] R. Eisenhitz and F. London, Z. Phys. **60**, 491 (1930).

[24] K. E. Riley, M. Pitoňák, P. Jurečka, and P. Hobza, Chem. Rev. **110**, 5023 (2010).

[25] A. Tkatchenko, L. Romaner, O. T. Hofmann, E. Zojer, C. Ambrosch-Draxl, and M. Scheffler, MRS Bulletin **35**, 435 (2010).

[26] J. Klimeš and A. Michaelides, J. Chem. Phys. **137**, 120901 (2012).

[27] P. L. Silvestrelli, Phys. Rev. Lett. **100**, 053002 (2008).

[28] P. L. Silvestrelli, J. Phys. Chem. A **113**, 5224 (2009).

[29] L. Andrinopoulos, N. D. M. Hine, and A. A. Mostofi, J. Chem. Phys. **135**, 154105 (2011).

[30] N. Marzari and D. Vanderbilt, Phys. Rev. B **56**, 12847 (1997).

[31] P. L. Silvestrelli, A. Ambrosetti, S. Grubisiĉ, and F. Ancilotto, Phys. Rev. B **85**, 165405 (2012).

[32] V. G. Ruiz, W. Liu, E. Zojer, M. Scheffler, and A. Tkatchenko, Phys. Rev. Lett. **108**, 146103 (2012).

[33] A. Tkatchenko, R. A. Di Stasio, R. Car, and M. Scheffler, Phys. Rev. Lett. **108**, 236402 (2012).

[34] M. W. Cole, H.-Y. Kim, and M. Liebrecht, J. Chem. Phys. **137**, 194316 (2012).

[35] P. L. Silvestrelli, K. Benyahia, S. Grubisiĉ, F. Ancilotto, and F. Toigo, J. Chem. Phys. **130**, 074702 (2009).

[36] A. Ambrosetti and P. L. Silvestrelli, Phys. Rev. B **85**, 073101 (2012).

[37] Y. Andersson, D. C. Langreth, and B. I. Lundqvist, Phys. Rev. Lett. **76**, 102 (1996).

[38] T. Brink, J. S. Murray, and P. Politzer, J. Chem. Phys. **98**, 4305 (1993).

[39] A. Bondi, J. Phys. Chem. **68**, 441 (1964).

[40] S. Grimme, J. Antony, T. Schwabe, and C. Mück-Lichtenfeld, Org. Biomol. Chem. **5**, 741 (2007); S. Grimme, J. Antony, S. Ehrlich, and H. Krieg, J. Chem. Phys. **132**, 154104 (2010).

[41] T. Thonhauser, V. R. Cooper, S. Li, A. Puzder, P. Hyldgaard, and D. C. Langreth, Phys. Rev. B **76**, 125112 (2007).

[42] N. D. Lang and A. R. Williams, Phys. Rev. B **18**, 616 (1978).

[43] N. W. Ashcroft and N. D. Mermin, *Solid State Physics* (Holt-Saunders International Editions, Philadelphia, 1976).

[44] P. Nordlander and J. Harris, J. Phys. C **17**, 1141 (1984); P.-A. Karlsson, A.-S. Mårtensson, S. Andersson, and P. Nordlander, Surf. Sci. **175**, L759 (1986).

[45] A. Tkatchenko and M. Scheffler, Phys. Rev. Lett. **102**, 073005 (2009).

[46] E. M. Lifshitz, Sov. Phys. JETP **2**, 73 (1956); E. Zaremba and W. Kohn, Phys. Rev. B **13**, 2270 (1976).

[47] F. Hanke, M. S. Dyer, J. Biörk, and M. Persson, J. Phys.: Condens. Matter **24**, 424217 (2012).

[48] S. Baroni *et al.*, www.quantum-espresso.org

[49] A. Ferretti *et al.*, www.wannier-transport.org

[50] Y. N. Zhang, F. Hanke, V. Bortolani, M. Persson, and R. Q. Wu, Phys. Rev. Lett. **106**, 236103 (2011).

[51] E. Abad, Y. J. Dappe, J. I. Martnez, F. Flores, and J. Ortega, J. Chem. Phys. **134**, 044701 (2011).

[52] J. L. Fajín, F. Illas, and J. R. B. Gomes, J. Chem. Phys. **130**, 224702 (2009).

[53] M.-S. Liao, C.-T. Au, and C.-F. Ng, Chem. Phys. Lett. **272**, 445 (1997).

[54] M. Karimi, D. Ila, I. Dalins, and G. Vidali, Surf. Sci. Lett. **239**, L505 (1990).

[55] P. L. Silvestrelli, F. Toigo, and F. Ancilotto, J. Phys. Chem. C **113**, 17124 (2009).

[56] A. Ambrosetti and P. L. Silvestrelli, J. Phys. Chem. C **115**, 3695 (2011).

[57] J. P. Perdew and Y. Wang, Phys. Rev. B **45**, 13244 (1992).

[58] M. Dion, H. Rydberg, E. Schröder, D. C. Langreth, and B. I. Lundqvist, Phys. Rev. Lett. **92**, 246401 (2004); G. Roman-Perez and J. M. Soler, *ibid.* **103**, 096102 (2009).

[59] K. Lee, É. D. Murray, L. Kong, B. I. Lundqvist, and D. C. Langreth, Phys. Rev. B **82**, 081101(R) (2010).

[60] O. A. Vydrov and T. Van Voorhis, Phys. Rev. A **81**, 062708 (2010).

[61] S. Andersson, M. Persson, and J. Harris, Surf. Sci. **360**, L499 (1996).

[62] E. Cheng, G. Mistura, H. C. Lee, M. H. W. Chan, M. W. Cole, C. Carraro, W. F. Saam, and F. Toigo, Phys. Rev. Lett. **70**, 1854 (1993).

[63] E. Hult and A. Kiejna, Surf. Sci. **383**, 88 (1997).

[64] E. Hult, P. Hyldgaard, J. Rossmeisl, and B. I. Lundqvist, Phys. Rev. B **64**, 195414 (2001).

[65] K. Watanabe and Y. Matsumoto, Surf. Sci. **454-456**, 262 (2000).

[66]A. A. Gokhale, J. A. Dumesic, and M. Mavrikakis, J. Am. Chem. Soc. **130**, 1402 (2008).
[67]G. Wang, L. Jiang, Z. Cai, Y. Pan, X. Zhao, W. Huang, K. Xie, Y. Li, Y. Sun, and B. Zhong, J. Phys. Chem. B **107**, 557 (2003).
[68]G.-C. Wang, S.-X. Tao, and X.-H. Bu, J. Catal. **244**, 10 (2006).
[69]L. Jiang, G.-C. Wang, Z.-S. Cai, Y.-M. Pan, and X.-Z. Zhao, J. Mol. Struct.: Theochem **710**, 97 (2004).
[70]T. D. Daff and N. H. de Leeuw, Chem. Mater. **23**, 2718 (2011).
[71]R. Nadler and J. F. Sanz, J. Mol. Model **18**, 2433 (2012).
[72]H. Ruuska, T. A. Pakkanen, and R. L. Rowley, J. Phys. Chem. B **108**, 2614 (2004).
[73]C. Au, J. Breza, and M. W. Roberts, Chem. Phys. Lett. **66**, 340 (1979).
[74]J. Carrasco, B. Santra, J. Klimeš, and A. Michaelides, Phys. Rev. Lett. **106**, 026101 (2011).
[75]M. Vanin, J. J. Mortensen, A. K. Kelkkanen, J. M. Garcia-Lastra, K. S. Thygesen, and K. W. Jacobsen, Phys. Rev. B **81**, 081408 (2010).
[76]N. Ferralis, H. I. Li, K. J. Hanna, J. Stevens, H. Shin, F. M. Pan, and R. D. Diehl, J. Phys.: Condens. Matter **19**, 056011 (2007).
[77]G. G. Kleiman and U. Landman, Solid State Commun. **18**, 819 (1976).
[78]Q.-L. Tang and Z.-X. Chen, Surf. Sci. **601**, 954 (2007).
[79]L. W. Bruch, Surf. Sci. **125**, 194 (1983).
[80]A. Derevianko, S. G. Porsev, and J. F. Babb, At. Data Nucl. Data **96**, 323 (2010).